ACS Catalysis

Research Article

pubs.acs.org/acscatalysis

Atomistic Engineering of Catalyst Precursors: Dynamic Reordering of PdAu Nanoparticles during Vinyl Acetate Synthesis Enhanced by Potassium Acetate

Elisabeth K. Hanrieder, Andreas Jentys, and Johannes A. Lercher*

Department of Chemistry and Catalysis Research Center, Technische Universität München, Lichtenbergstraße 4, 85747 Garching, Germany

Supporting Information

ABSTRACT: The presence of potassium acetate (KOAc) on bimetallic PdAu catalysts increases the rate of reaction for vinyl acetate (VA) formation from ethene and acetic acid by a factor of 10 and the selectivity by 20%. The dynamic transitions of typical supported catalyst precursors with an atomic Pd/Au ratio of 2/1 were explored during synthesis in the presence and absence of KOAc. The dopant induces reordering of PdAu toward a Pd_1Au_1 phase, while Au-enriched $Pd_{40}Au_{60}$ bimetallic particles form primarily in the absence of KOAc. Pd−acetate species are generated via leaching of Pd from PdAu precursor particles during the reaction. These species are $Pd_3(OAc)_6$ and $Pd_2(OAc)_4$ in the absence of KOAc and $K_2Pd_2(OAc)_6$ in the presence of KOAc. Palladium in $K_2Pd_2(OAc)_6$ can be readily reduced by C_2H_4 to Pd^0, while $Pd_3(OAc)_6$, which contains more stable, bridged acetate ligands remains stable. Reduced Pd either forms dispersed Pd^0 or is incorporated into the metal particles. KOAc enhances rates and selectivity to VA by stabilizing, on the one hand, active Pd species at the bimetallic surface. On the other hand, KOAc enriches acetic acid close to the surface and forms Pd surface acetates, postulated to enhance the rate and the selectivity to VA by suppressing ethylene adsorption and oxidation.

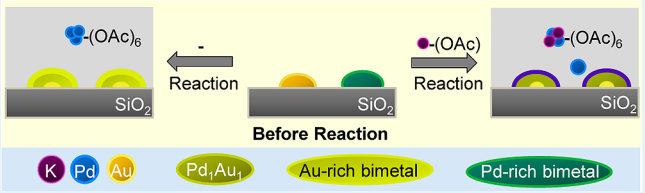

KEYWORDS: *silica-supported palladium gold alloy catalysts, KOAc promoter, (in situ) FTIR, absorption/extinction coefficient, XRD*

1. INTRODUCTION

The heterogeneously catalyzed acetoxylation of ethene to vinyl acetate (VA) over silica-supported bimetallic palladium gold (PdAu) particles promoted with potassium acetate (KOAc) is a structure-sensitive reaction.[1,2] The active sites consist of two isolated Pd surface atoms separated by Au atoms (Figure 1).[3]

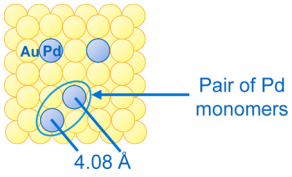

Figure 1. Pair of Pd monomers on e.g. Au(100), proposed as an active site for VA synthesis.[3]

The active surface species are typically formed under the influence of the reactant atmosphere,[4] and we have recently shown that KOAc-promoted Pd_xAu_y particles restructure into bimetallic Pd_1Au_1 and Pd particles under reaction conditions.[5] The role of alkaline acetate promoters, which improves the overall activity and selectivity of the catalyst, is hardly understood.[6]

The most widely held explanation attributes the promoting effect of alkali metals to their electronic influence on Pd. The cationic promoter's[7,8] hybridization of its s and p energy levels with the metal electronic states broadens and shifts their band positions relative to the Fermi level. This process is determined by the competition between the tendency to fill the valence shell and the electron affinity of the metal. Consequently, electrons are partially transferred from the alkali-metal cation to the metal, creating a surface dipole.[9] In accordance with this interpretation, Gravelle-Rumeau-Maillot et al.[10] reported that the initial heat of adsorption of CO increased slightly (ca. 10%) in the presence of K^+ and Na^+, which is also reflected in the lower wavenumbers of adsorbed CO. While such promotion is certainly present in PdAu/KOAc catalysts, the existence of the liquidlike acetic acid (AcOH) layer on the catalyst under reaction conditions[11] leads to a more complex situation. Strong interactions of acetic acid and acetate ions with Pd allow leaching it from bimetallic particles as Pd acetate,[12] which affects the reordering of PdAu particles.

The mobile Pd acetate in liquid acetic acid exists as a monomer, dimer, and trimer. The concentrations of these species are controlled by the addition of alkali-metal acetates (MOAc) (eqs 1 and 2).[13−15] With increasing MOAc concentration, trimeric $Pd_3(OAc)_6$[16−18] is converted into active dimeric $Pd_2(OAc)_6^{2-}$, while presumably inactive monomeric $Pd(OAc)_4^{2-}$ was not

Received: June 2, 2015
Revised: August 20, 2015
Published: August 24, 2015

DOI: 10.1021/acscatal.5b01140
ACS Catal. 2015, 5, 5776−5786

$$2Pd_3(OAc)_6 + 6MOAc \rightleftharpoons 3M_2Pd_2(OAc)_6 \quad (1)$$

$$M_2Pd_2(OAc)_6 + 2MOAc \rightleftharpoons 2M_2Pd(OAc)_4 \quad (2)$$

formed under the conditions of the homogeneous catalytic conversion of ethylene.[16,19]

In addition, PdAu particles change dynamically under working conditions, as Pd leaches into AcOH and binds to or reacts with the adsorbed molecules. These variations in structure and chemical composition, induced by reactants and intermediates, control the overall activity and selectivity in VA synthesis. Thus, atomistic information is required to analyze the nature, geometry, and environment of the active sites during catalysis.[20] Given the central role of the KOAc promoter, we explore in this contribution its impact on the reordering processes of PdAu particles and in turn on activity and selectivity.

2. EXPERIMENTAL SECTION

2.1. Synthesis. $PdAu/SiO_2$ catalysts were synthesized with a molar Pd/Au ratio of 2.0 to achieve equal amounts of Pd in the bimetallic Pd_1Au_1 particles and as dispersed Pd species during reaction.[5] This Pd distribution is the most appropriate way to study the heterogeneous pathway (on the PdAu surface) in parallel to the homogeneous pathway to VA (via Pd acetate species). Catalysts were prepared via incipient wetness impregnation according to ref 21. Aqueous solutions of $HAuCl_4$ and $PdCl_2$ were impregnated on mesoporous SiO_2 (HDK, 200 m^2/g, 1.1 mL/g) followed by precipitation of Pd^{2+} and Au^{3+} ions with sodium carbonate and washing with ammonia solution (pH 8) to remove chloride ions from the metal precursors. The $PdAu/SiO_2$ precursor was reduced under flowing H_2 (100 mL/min) at 300 °C for 1 h with a heating rate of 5 °C/min. The Pd as well as the Au loading was ~1.5 wt %, corresponding to a molar PdAu ratio of 2.0. The catalyst was impregnated with 5 wt % K^+, whereas samples for IR studies were impregnated with 2 wt % of K^+ using an aqueous solution of KOAc. A physical mixture between monometallic Pd/SiO_2 and Au/SiO_2 was prepared using 3 wt % Pd/SiO_2 and Au/SiO_2 in a molar ratio of 2/1 impregnated with 5 wt % KOAc. The term "$PdAu/SiO_2$" refers to the unpromoted and "$PdAu/KOAc/SiO_2$" to the promoted PdAu catalyst. The physical mixture of monometallic Pd and Au promoted with KOAc is called "$(Pd+Au)/KOAc/SiO_2$". Reference catalysts were impregnated with $Pd(OAc)_2$ (3 wt % Pd) and with KOAc (5 wt % K^+).

2.2. X-ray Powder Diffraction. X-ray powder diffraction measurements were conducted on a Philips X'Pert Pro System using Cu Kα radiation (0.154056 nm) generated at 45 kV and 40 mA. The samples were mounted on a rotating powder holder and measured in a 2θ range of 5−70° with a step size of 0.017° s^{-1}. Peak fitting was performed with High Score Plus software using the crystallographic open database (COD) to derive the exact peak positions and to calculate the alloy compositions using Vegard's rule.[22]

2.3. Low-Temperature IR Spectroscopy during CO Adsorption. The infrared spectra were recorded on a Vertex 70 spectrometer from Bruker Optics with a resolution of 4 cm^{-1}. The samples were prepared as self-supporting wafers (~10 mg/cm). The samples were first activated under vacuum (better than 1×10^{-7} mbar) at 300 °C (heating rate 5 °C/min) for 1 h and reduced in 1000 mbar of H_2 at 300 °C (heating rate 5 °C/min). After reduction, the samples were outgassed at 300 °C under vacuum for 30 min and cooled to −150 °C with liquid nitrogen in 3 mbar of He to maintain the temperature at −150 °C. After the spectrum of the activated sample was recorded, 1 mbar of CO and 50 mbar of He were introduced to the system. Spectra were collected during CO adsorption at −150 °C until the adsorption desorption equilibrium was reached. All IR spectra were normalized to the integrated area of the Si−O overtones of the activated sample between 2107 and 1741 cm^{-1}. The contributions of the individual CO bands were evaluated by band fitting, applying a mixed 50/50 Gaussian−Lorentzian function in the region between 2140 and 2000 cm^{-1} using the software Grams AI. In order to extract the KOAc-induced changes in the PdAu surface composition, band positions for CO adsorbed on either Pd or Au on fresh $PdAu/KOAc/SiO_2$ were fitted considering the CO band positions of $Pd/KOAc/SiO_2$ and $Au/KOAc/SiO_2$.

2.4. In Situ IR Spectroscopy. Infrared spectra of the samples in continuous flow were collected with a resolution of 4 cm^{-1} on a Thermo Fisher Nexus instrument. The samples were pressed into self-supporting wafers (10 mg/cm^2), cut in half, and placed in a flow IR cell designed by Mirth et al.[23] The cell was vertically moved to measure IR spectra of either the wafer or the gas phase present inside the cell through the empty section in the upper half. This enabled us to subtract the contributions of the gas phase (which is significant at a pressure of 9 bar) from the spectra of the adsorbed species measured. Prior to adsorption, samples were reduced at 250 °C (heating rate 5 °C/min) in H_2 followed by N_2. Acetic acid was added using a temperature-controlled saturator, and oxygen and ethylene were mixed into the N_2 carrier gas stream via mass flow controllers at 150 °C and 9 bar.

2.5. Catalytic Reactions. The activity of the catalysts for VA synthesis was studied in a 6-fold reactor setup at 150 °C, at 9 bar of total pressure and a gas composition of 60 vol % of C_2H_4, 13 vol % of AcOH, and 4.5 vol % of O_2 in N_2. SiC (355−500 μm) was used as inert diluent to maintain a constant temperature over the catalyst bed (180−250 μm). The diluent/catalyst ratio was chosen to be 10/1. The product stream was analyzed using a GC (Model 2014 from Shimadzu), equipped with a Haysep Q, a molecular sieve column, and a TCD detector.

3. RESULTS AND DISCUSSION

3.1. Vinyl Acetate Synthesis on KOAc-Promoted and -Unpromoted $PdAu/SiO_2$. The influence of KOAc on the activity and selectivity of bimetallic PdAu catalysts in VA synthesis was studied during continued operation. The formation rates and selectivities of $PdAu/SiO_2$ and $PdAu/KOAc/SiO_2$ are compiled in Figure 2. The slight decrease in selectivity during the initial induction period of ~1000 min can be related to the increase in activity of $PdAu/KOAc/SiO_2$. During this time, the PdAu particles undergo severe restructuring processes by leaching Pd^{2+} from the bimetallic phase. In parallel, the overall activity increases as more active but less selective PdAu surface arrangements with a lower Pd/Au ratio are generated. After this induction period, $PdAu/KOAc/SiO_2$ deactivated only by ~4%; the selectivity increased marginally to 95%, in good agreement with refs 24−26. In contrast, the activity and selectivity of (potassium free) $PdAu/SiO_2$ decreased considerably, leading to almost complete deactivation after 6000 min.[27]

DOI: 10.1021/acscatal.5b01140
ACS Catal. 2015, 5, 5776−5786

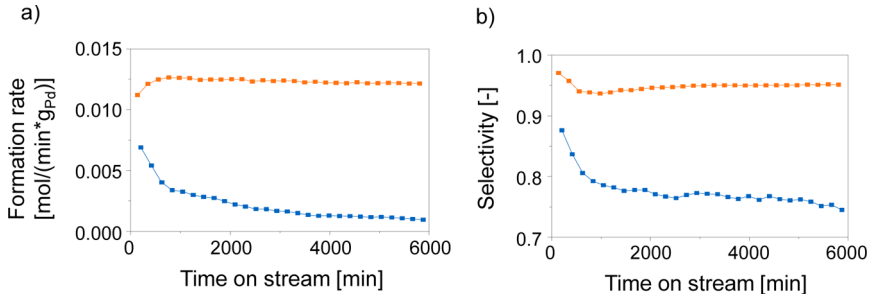

Figure 2. (a) Formation rates normalized to the concentration of Pd in the bimetallic phase and (b) selectivities for $PdAu/SiO_2$ (blue) and $PdAu/KOAc/SiO_2$ (orange) with time on stream. Reaction conditions: 60 vol % of C_2H_4, 13 vol % of AcOH, 4.5 vol % of O_2, balance N_2; total pressure, 8.8 bar; temperature, 150 °C.

3.2. KOAc Enhancement of Reactive Reordering of PdAu Particles in the Heterogeneous Pathway to VA Synthesis.

3.2.1. Effect of KOAc on the Pd_xAu_y Bulk Composition. To investigate the effect of KOAc on the bulk composition of the Pd_xAu_y particles during time on stream, X-ray diffractograms for fresh and used catalysts with and without KOAc were compared between 36 and 42° 2θ (Figure 3).

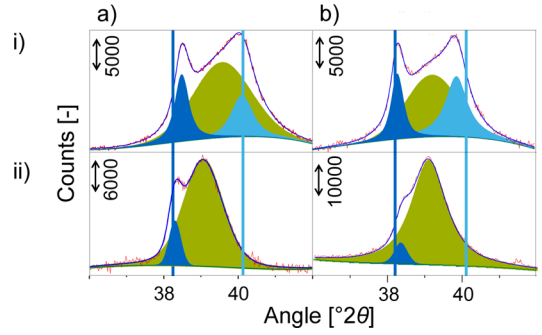

Figure 3. XRD profiles for 111 planes (i) before and (ii) after reaction for $PdAu/SiO_2$ (a) and $PdAu/KOAc/SiO_2$ (b). The bimetallic phase of the 111 plane is located between those of the pure metals: Au(111) (2θ = 38.3°) (darker blue line); Pd(111) (2θ = 40.1°) (brighter blue line).

The positions of Au(111) at 38.3° and Pd(111) at 40.1° indicated by darker blue and brighter blue lines, respectively, were calculated from fcc lattice constants reported in the COD database (a_{Au} = 4.060 Å and a_{Pd} = 3.890 Å). The Pd_xAu_y alloy compositions of fresh and used samples, derived from the fitted peak positions applying Vegard's law,[22] are compiled in Table 1.

Table 1. Alloy Compositions of $PdAu/SiO_2$ and $PdAu/KOAc/SiO_2$ before and after Reaction Determined by XRD

	$PdAu/SiO_2$	$PdAu/KOAc/SiO_2$
before reaction	Pd_7Au_{93}, $Pd_{69}Au_{31}$, $Pd_{98}Au_2$	Au_{100}, $Pd_{54}Au_{46}$, $Pd_{89}Au_{11}$
after reaction	Au_{100}, $Pd_{40}Au_{60}$	Pd_4Au_{96}, $Pd_{47}Au_{53}$

The potassium-free $PdAu/SiO_2$ catalyst (Figure 3ai) before reaction consisted of Au- and Pd-rich particles with average compositions of Pd_7Au_{93}, $Pd_{98}Au_2$, and $Pd_{69}Au_{31}$. The peaks had an asymmetric shape, indicating a distribution of particles with varying composition before reaction.

After 6000 min time on stream (Figure 3aii), a small fraction of monometallic Au particles (or Au-rich core−shell particles[28,29]) remained, while diffraction lines of monometallic Pd particles were not observed. The main fraction of $Pd_{40}Au_{60}$ contained significantly less Pd than expected from the overall Pd/Au ratio of 2. Thus, a considerable fraction of Pd (~63%) is concluded to be XRD amorphous: i.e., in the form of very small Pd^0 particles or/and dissolved Pd acetate.[4,5,30]

On KOAc-promoted $PdAu/SiO_2$ (Figure 3bi) the composition of the X-ray crystalline bimetallic PdAu particles changed from 2/1 ($Pd_{69}Au_{31}$) to approximately 1/1 ($Pd_{54}Au_{46}$) already upon impregnation with KOAc. We conclude that this is induced by the formation of Pd acetate. Such surface chemistry between Pd and KOAc was also observed by EPR.[31] It is hypothesized that during the impregnation process partly oxidized Pd interacts with the acetate anions, leading in turn to the removal of Pd from the bimetallic particles after impregnation.

After reaction, $PdAu/KOAc/SiO_2$ (Figure 3bii) mainly consisted of $Pd_{47}Au_{53}$ particles (close to a Pd_1Au_1 phase) and a small fraction of Pd_4Au_{96}, likely located in the particle core.[28,29] The content of dispersed Pd species was estimated to be 53% of the total Pd loading, assuming that most of the Au is alloyed with Pd.[28,30] After reaction, the fraction of dispersed Pd was lower for the promoted PdAu catalyst than for the unpromoted catalyst, which indicates that the equilibrium between leached Pd and the bimetallic PdAu phase is affected by the presence of KOAc. Thus, KOAc not only removes Pd from bimetallic PdAu particles but also stabilizes the bimetallic Pd_1Au_1 phase during the reaction. In these used catalysts, the full width at half-maximum is higher for $PdAu/SiO_2$ than for $PdAu/KOAc/SiO_2$, indicating smaller PdAu particles on $PdAu/SiO_2$. This is probably due to the higher concentration of dispersed Pd leached from the bimetallic particles on $PdAu/SiO_2$ and due to the absence of KOAc, which induces particle agglomeration on $PdAu/KOAc/SiO_2$.[32] The loss of Pd under the reaction conditions appears to be inevitable and may be retarded by the presence of KOAc, but not stopped (after 6000 min $Pd_{47}Au_{53}$ was observed with KOAc-promoted catalysts while $Pd_{40}Au_{60}$ was observed in the absence of KOAc). This is clearly demonstrated by a reactor study over 14 months, which reported $Pd_{38}Au_{62}$[30] as a thermodynamically stable alloy having a formation enthalpy of −7.8 kJ/mol.[33−35] Although the PdAu surface structure is particularly important for catalysis, the bulk phase composition is also substantial for VA synthesis, as it is directly connected to the surface composition by dynamic reordering and leaching Pd^{2+} into the acetic acid film. Catalysts with an overall Pd/Au ratio of 1 showed a pronounced loss in selectivity and activity with time on stream in comparison to Pd-rich samples, since Pd_1Au_1 particles initially present will also leach Pd in form of Pd^{2+} to generate

DOI: 10.1021/acscatal.5b01140
ACS Catal. 2015, 5, 5776−5786

Au-enriched particle surfaces that favor the combustion of C_2H_4 to CO_2 over the formation of VA. In contrast to Pd-enriched surfaces, Au-enriched surfaces exhibit low concentrations of Pd monomers (active sites) but adsorption sites for C_2H_4, which react to give CO_2 with oxygen adsorbed on Pd sites.

In order to confirm the dynamic exchange of Pd between solved or dispersed Pd^0 and Pd in bimetallic PdAu particles, a physical mixture, (Pd+Au)/KOAc/SiO_2, of monometallic Au and Pd particles (Figure 4a) was used as catalyst (Figure 4b).

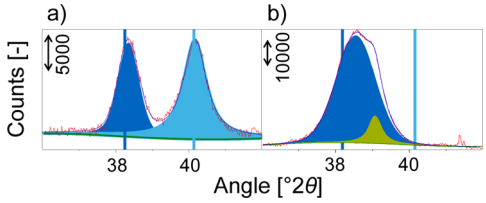

Figure 4. XRD profiles for the 111 plane of (Pd+Au)/KOAc/SiO_2 (a) before and (b) after reaction. The bimetallic phase is located between the positions of the pure metals: Au(111) (2θ = 38.3°) (darker blue line), Pd(111) (2θ = 40.1°) (brighter blue line).

The XRD peaks of Au(111) and Pd(111) in the physical mixture before reactions were shifted by 0.175 and 0.080° 2θ to higher angles with respect to the reference materials (darker blue and brighter blue lines), indicating shorter distances between metal atoms in the small metal particles.

During the reaction, (Pd+Au)/KOAc/SiO_2 (Figure 4b) underwent severe reordering, as the initial peaks for Au_{100} and Pd_{100} disappeared. Particles of $Pd_{45}Au_{55}$ and $Pd_{15}Au_{85}$ formed, as well as a major part of XRD-invisible Pd acetate or Pd^0 (sub) nanoparticles (~91%). The formation of bimetallic $Pd_{15}Au_{85}$ is attributed to the incorporation of Pd^0 into Au particles, which indicates reversibility between oxidative leaching and reductive reincorporation. The formation of the bimetallic phase on (Pd+Au)/KOAc/SiO_2 confirms that an oxidative dissolution of Pd^{2+}, a transfer of Pd^{2+} to pure Au particles in the AcOH layer, and a reduction of Pd^{2+} to incorporate Pd^0 in Au particles are possible under the reaction conditions of the VA synthesis. In situ reduction of Pd^{2+} in the presence of Au nanoparticles resulted in catalytically active AuPd bimetallic catalysts.

TEM studies showed that the average particle size of (Pd+Au)/KOAc/SiO_2 decreased from initially 3.5 nm to 1−2 nm with agglomerates in the range of ~5−12 nm after reaction. Particle sizes below 1.0 nm were not observed (Figure S1 in the Supporting Information). This suggests that Pd particles dissolved in AcOH (1−2 nm particles), while Au particles grew in the presence of KOAc (5−12 nm particles) (Figure 4b).[36−38] The activity normalized to the total Pd concentration and the selectivity of (Pd+Au)/KOAc/SiO_2 are comparable to those for PdAu/KOAc/SiO_2 (Figure S2 in the Supporting Information).

3.2.2. Effect of KOAc on the PdAu Surface Composition during VA Synthesis. While the preceding experiments have shown how the nanoparticles reorganize during catalysis, the surface composition may be very different. In order to explore this, we have used the IR spectra of adsorbed CO after removing the layer of KOAc or Pd acetate by washing the material with water, restoring the accessibility of the surface. Leaching of Au species by this procedure was not detected.

The IR spectra of 1.0 mbar of CO adsorbed on SiO_2 are shown in Figure S3 in the Supporting Information. At −150 °C, CO adsorbed on the OH groups of SiO_2 (2157 cm^{-1})[39,40] and on cations (2184 cm^{-1}).[41,42] The band at 2135 cm^{-1} is assigned to CO physically adsorbed on the surface of SiO_2.[43,44] Stretching bands of CO adsorbed on Au or Pd nanoparticles (Figure 5i)

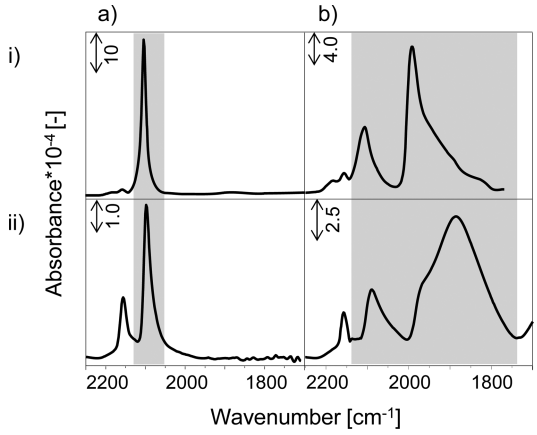

Figure 5. IR spectra of adsorbed CO at −150 °C and 1.0 mbar partial pressure of CO on (i) parent and (ii) KOAc promoted monometallic Au/SiO_2 (a) and Pd/SiO_2 (b).

above 2000 cm^{-1} are attributed to linearly adsorbed CO and bands below 2000 cm^{-1} to CO adsorbed in a bridged and 3-fold-hollow mode.[39,45,46] On Au/SiO_2, CO was only adsorbed linearly (2104 cm^{-1}, Figure 5ai),[47−50] while on Pd, bands of linear and bridge-bonded CO were observed at 2109 and 1991 cm^{-1}, respectively (Figure 5bi).[48,51−53]

The presence of KOAc on Au/SiO_2 (Figure 5aii) and on Pd/SiO_2 (Figure 5bii) led to a decrease in the wavenumbers of linearly adsorbed CO by 6 cm^{-1} on Au and by 17 cm^{-1} on Pd. The larger red shift of CO on Pd/KOAc/SiO_2 indicated a more pronounced electronic impact of KOAc on Pd than on Au. Alkali-metal ions as well as neutral alkali metals were shown to both act as electron donors, as they bear a positive charge, δ^+, when they are adsorbed on a metal. In both cases, the CO frequency shifted to lower wavenumbers.[9,10,42,54−59] In agreement with these experiments, we assign the downshift of ν(CO) on PdAu/KOAc in comparison to PdAu to the presence of electron-donating K^+. K^+ increased the electron density on Pd and Au, enhancing the electron back-donation from the metal into the nonbonding $2\pi^*$ orbital of CO. This causes weakening of the CO bond, reflected in the lower wavenumbers.[60−63] The intensities of the CO bands on Pd/SiO_2 and Au/SiO_2 were significantly lower in the presence of K^+, suggesting that K^+ decreases the accessibility of Pd and Au for CO. On Pd/SiO_2 a redistribution from linear to bridged adsorbed CO was observed in the presence of the promoter, which is attributed to the formation of Pd-CO-K^+ (band at 1850 cm^{-1}) from linear Pd-CO species.[10,54,59,64−67] Bands of Pd-CO-K^+ and of bridged CO with a pronounced downshift may overlap in this region.

While the experiments demonstrate qualitatively that K^+ electronically influences the monometallic nanoparticles, a more detailed analysis requires exploring the changes also including the structural modifications induced by the promoter on bimetallic PdAu particles. The shift in the CO wavenumber as a function of the surface PdAu geometry (ensemble effect)[48] is inevitably related to the electronic interaction between the two metals.[68−71] Alloying Pd with Au tends to shift the electron density toward the element with the larger fraction of empty

DOI: 10.1021/acscatal.5b01140
ACS Catal. 2015, 5, 5776−5786

valence states.[72] Lee et al. suggested that Au gains sp electrons and loses d electrons whereas Pd loses sp electrons and gains d electrons.[73] As the reactivity is mainly determined by the d orbitals, the increase in the electron density in Pd allows the stronger electron donation into the antibonding π^* orbitals of CO (shift of the CO stretching vibration to lower wavenumbers).[48] In contrast, the band of linearly adsorbed CO on Au in proximity to Pd shifts to higher wavenumbers, as the electron density in the d bands of Au decreases by the interaction with Pd. (See the supporting information of ref 5 for the CO band transitions of CO adsorbed on pure Au/SiO_2 and Pd/SiO_2 in comparison to bimetallic $PdAu/SiO_2$.) Figure 6

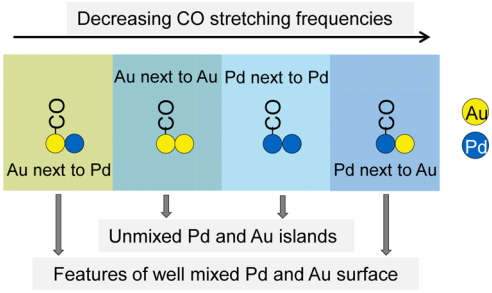

Figure 6. Linearly adsorbed CO in different PdAu environments.

schematically illustrates the adsorption of CO on Pd and Au in the different environments. It should be noted in passing that such electronic effects may be counteracted by a higher concentration of CO leading to an upward shift of the ν(C═O) band by CO dipole−dipole coupling. Dilution of Pd by Au reduces the probability of such dipole−dipole coupling.

The strong interaction of Pd with the acetate anion makes it likely that KOAc induces surface segregation in PdAu alloys. In the absence of external factors it has been predicted[74] that Au segregates to the surface,[50,75−79] because the surface free energy of Pd (2.043 J/m^2)[80] is higher than that of Au (1.626 J/m^2).[81] However, the stronger interaction of Pd with the acetate anion is expected to reverse this effect.

The relative intensities of the bands of linear and multiply bonded CO as well as their wavenumbers allow us to characterize the degree of surface intermixing.[41] The probability of CO to adsorb in a multifold position is enhanced for larger Pd ensembles, and thus, the ratio of the band areas of linear to multifold adsorbed CO decreases. The surface concentrations as well as the fractions of linearly adsorbed CO (Table 2) were calculated from the integral areas of the bands using absorption coefficients ε determined from the adsorption of CO on monometallic Au/SiO_2 and Pd/SiO_2. In order to calculate ε_{linear}(Pd), a $\varepsilon_{linear}/\varepsilon_{bridged}$ ratio of 85×10^7 to 3.3×10^7 cm/mol was assumed for Pd using the absorption coefficients of Vannice et al.[45] (Supporting Information).

The spectra of CO adsorbed on fresh and used as well as on parent and KOAc-containing $PdAu/SiO_2$ are shown in Figure 7.

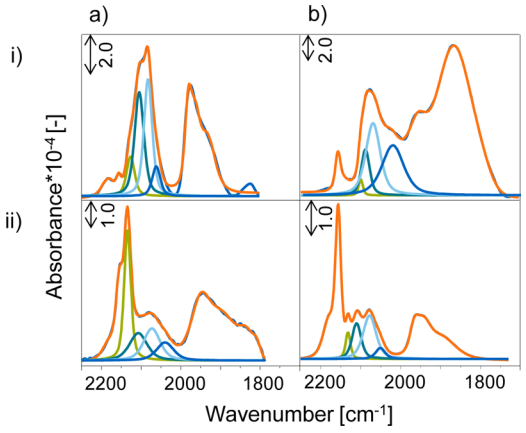

Figure 7. IR spectra of adsorbed CO at −150 °C and 1.0 mbar partial pressure of CO before (i) and washed after reaction (ii) on $PdAu/SiO_2$ (a) and $PdAu/KOAc/SiO_2$ (b). Green lines represent CO on Au and blue lines CO on Pd.

On the parent fresh catalyst (Figure 7ai), two bands for linearly bound CO on Au (2128 and 2106 cm^{-1})[44] and linearly bound CO on Pd (2084 and 2063 cm^{-1}) were observed. The band at 2128 cm^{-1} is attributed to CO on Au surrounded by Pd atoms (linear CO on "Au next to Pd") and the band at 2106 cm^{-1} is assigned to CO linearly bound on Au in proximity to Au atoms (linear CO on "Au next to Au"). The band at 2084 cm^{-1} is associated with CO chemisorbed on larger Pd islands (linear CO on "Pd next to Pd") and the band at 2063 cm^{-1} with linear CO adsorption on Pd surrounded by Au (linear CO on "Pd next to Au").[82] Before reaction the surface of this catalyst (Figure 7ai) consisted mainly of larger Au and Pd domains, as concluded from strong bands at 2106 cm^{-1} (8.7×10^{-6} mol/g, 33%) and 2084 cm^{-1} (12×10^{-6} mol/g, 45%). The intensities of the bands at 2128 and 2063 cm^{-1} (well-mixed PdAu surface) were low (2.9×10^{-6} mol/g (11%) and 3.0×10^{-6} mol/g (11%), respectively). The overall Pd/Au ratio of 1.28 indicates a slight Pd surface enrichment, which is attributed to a preferred stabilization of Pd via the interaction with H_2 during reduction.

The presence of KOAc caused the fraction of "Au next to Pd" and "Au next to Au" to decrease (from 2.9×10^{-6} mol/g (11%) to 0.9×10^{-6} mol/g (2%) and from 8.7×10^{-6} mol/g (33%) to 4.9×10^{-6} mol/g (12%)): i.e., the surface concentration of Au decreased. The fraction of "Pd next to Au" consequently increased significantly from 3.0×10^{-6} mol/g (11%) to 18×10^{-6} mol/g (43%). The pronounced shift of the band for CO on "Pd next to Au" to 2023 cm^{-1} indicates that this change

Table 2. Surface Concentrations (10^{-6} mol/g) and Corresponding Fractions (%) in Parentheses of CO Adsorbed on the Catalysts before (B) and after Reaction (A)

	concentration [10^{-6} mol/g] ([%])				ratio [−]	
sample	Au next to Pd	Au next to Au	Pd next to Pd	Pd next to Au	linear/bridged CO	Pd/Au
$PdAu/SiO_2$_B	2.9 (11)	8.7 (33)	12 (45)	3.0 (11)	29.0	1.28
$PdAu/KOAc/SiO_2$_B	0.9 (2)	4.9 (12)	18 (43)	18 (43)	11.2	6.30
$PdAu/SiO_2$_A	6.6 (36)	3.5 (19)	5.3 (28)	3.1 (17)	16.5	0.83
$PdAu/KOAc/SiO_2$_A	0.6 (10)	1.6 (24)	3.6 (56)	0.7 (10)	20.5	1.97

DOI: 10.1021/acscatal.5b01140
ACS Catal. 2015, 5, 5776−5786

partially arises from CO adsorbed on the XRD amorphous Pd-KOAc species deposited on top of Au or mixed PdAu surfaces. Thus, the increase of this fraction cannot be directly assigned to the intermixing within a bimetallic particle. However, the surface concentration of "Pd next to Pd" increased from 12 × 10^{-6} mol/g to 18 × 10^{-6} mol/g, the overall surface Pd/Au ratio increased from 1.28 to 6.30, and the ratio of linear to bridged adsorbed CO decreased from 29.0 to 11.2 in the presence of KOAc. Thus, Pd is concluded to migrate from the bulk to the surface.

XRD (Figure 3) indicates that the presence of KOAc removed some Pd from the alloy, changing its nominal composition from $Pd_{69}Au_{31}$ to $Pd_{54}Au_{46}$ as well as leading to the formation of the Pd−KOAc adlayer. The high concentration of CO adsorbed on PdAu/KOAc/SiO_2 (Figure 7bi) is attributed to a much higher surface concentration of Pd, resulting from the segregation of Pd to the surface as well as from the presence of the acetate adlayer. The migration of Pd to the surface of the bimetallic particles accelerated the leaching of Pd and the associated reorganization of PdAu nanoparticles. The small fraction of Pd_4Au_{96} is attributed to excessive leaching in individual particles or to the formation of a core in a more complex particle.

On fresh and used PdAu/SiO_2 the fractions of unmixed "Au next to Au" decreased from 8.7 × 10^{-6} mol/g (33%) to 3.5 × 10^{-6} mol/g (19%) and "Pd next to Pd" decreased from 12 × 10^{-6} mol/g (45%) to 5.3 × 10^{-6} mol/g (28%), indicating a better intermixed, but overall Au rich, PdAu surface after reaction (Pd/Au ratio of 0.83). In accordance, the fraction of mixed "Au next to Pd" increased from 2.9 × 10^{-6} mol/g (11%) to 6.6 × 10^{-6} mol/g (36%), whereas the fraction of mixed "Pd next to Au" remained at ∼3 × 10^{-6} mol/g (11%, 17%) on fresh and used PdAu/SiO_2 (Figure 7ai,aii).

Assuming that "Pd next to Au" and "Au next to Pd" are neighbors in the same surface plane of the particle, both bands would have been expected to change in parallel. The absence of this observation guides us, therefore, to the conclusion that the outer layer of the bimetallic particles consists of mainly Au atoms, while Pd atoms are in a subsurface layer and, thus, are not accessible for CO. It should be noted in passing that this observation agrees well with ion scattering results of Swartzfager et al.[83] Figure 8 shows an illustration of the hypothetical particle with an Au-enriched surface and a Pd-enriched subsurface layer.

Figure 8. Schematic intersection of a PdAu particle on used PdAu/SiO_2 with an Au-enriched surface and a Pd-enriched subsurface layer.

In a related experiment, it was observed that on a used, unwashed PdAu/SiO_2 sample (Figure S4 in the Supporting Information) CO adsorption gives a lower Pd/Au ratio (0.62) in comparison to that on the sample after the removal of acetic acid by washing (0.83). It is speculated that water induced surface segregation by a strong interaction with Pd.

The Au surface enrichment is hypothesized to be the reason for the low activity of unpromoted PdAu/SiO_2, as the generally proposed active site consists of two Pd atoms on a well-intermixed PdAu surface.[77,84,85] The surface concentration of Pd on used PdAu/SiO_2 of 0.62 is too low for effectively coupling vinyl and acetate species on considering this reaction as the rate-determining step in VA synthesis. The initial high activity of PdAu/SiO_2 (Figure 2a) is exclusively related to the high Pd/Au surface ratio of 1.28, as rate-enhancing factors such as KOAc are absent and reactant concentrations remain constant. The drastic activity decrease is caused by Pd leaching lowering the Pd/Au surface ratio. This hinders the coupling of vinyl with acetate species but favors their decomposition to CO_2 and H_2O, thus lowering the overall selectivity. The selectivity of industrial catalysts critically depends on the overall molar Pd/Au ratio and thus on the PdAu surface composition in equilibrium with leached Pd species.

In contrast, the presence of the KOAc promoter leads to an enrichment of Pd on PdAu/KOAc/SiO_2 (Pd/Au = 1.97) in comparison to unpromoted PdAu/SiO_2 (Pd/Au = 0.83) after reaction. The Pd/Au ratio of PdAu/KOAc/SiO_2 decreased from 6.30 before the reaction to 1.97 after the reaction, indicating that surface Pd leached into the acetic acid layer under reaction conditions. The low concentration of adsorbed CO on used PdAu/KOAc/SiO_2 (Figure 7bii) in comparison to used PdAu/SiO_2 (Figure 7aii) is attributed to the removal of the Pd−KOAc adlayer by washing.

The high activity of PdAu/KOAc/SiO_2 is attributed, in turn, to the fact that KOAc stabilizes a sufficient concentration of active Pd sites on the bimetallic PdAu surface. Interestingly, the high ratio of linear to bridged CO on PdAu/KOAc/SiO_2 (20.5) after the reaction points to the presence of "optimized" Pd/Au ensembles (Figure 1). These ensembles reduce the probability of the direct combustion of adsorbed ethylene or acetic acid, thus leading to higher VA selectivity.

3.3. Formation of Reactive Pd Species in the Presence and Absence of KOAc. After the reaction PdAu/SiO_2, PdAu/KOAc/SiO_2 ,and (Pd+Au)/KOAc/SiO_2 samples contained 63%, 53% and 92% of XRD amorphous Pd species. X-ray diffraction of fresh and used (Pd+Au)/KOAc/SiO_2 indicated an equilibrium between leached Pd^{2+} (from Pd_xAu_y) and reincorporated Pd^0 (into Pd_xAu_y). As dissolved Pd^{2+} complexes are generally accepted as active sites for the molecularly catalyzed VA synthesis,[86] the contribution of this route cannot at present be excluded.

3.3.1. Surface Structures in the Presence and Absence of KOAc. In order to understand the presence of reactive Pd intermediates on Pd_xAu_y better and to study their interaction with KOAc during the reaction, AcOH and AcOH/O_2 were adsorbed on Pd/SiO_2 and on PdAu/KOAc/SiO_2 under reaction conditions. The changes in the IR spectrum (1900−1300 cm^{-1}) of Pd/SiO_2 after AcOH adsorption are shown in Figure 9a.

AcOH adsorbed in monomeric (ν(C═O) 1767 cm^{-1}) and dimeric forms (ν(C═O) 1737 cm^{-1}) (Figure 10).[87−89] Small concentrations of acetic acid were converted into silyl acetates by esterification of terminal Si−OH groups,[90,91] as characterized by the asymmetric and symmetric carboxylate stretching vibrations at 1613 and 1586 cm^{-1} (ν_{as}(COO)) as well as at 1457 and 1434 cm^{-1} (ν_s(COO)). The band at 1380 cm^{-1} is assigned to the symmetric CH_3 bending vibration (Figure 9a).[87,92] The presence of Pd acetate during AcOH adsorption on the fully reduced Pd/SiO_2 is excluded, because oxidizing reactants were absent.[12,93,94]

The difference between the IR spectra of AcOH adsorbed in the presence and absence of O_2 on Pd/SiO_2 is shown in Figure 9b in order to illustrate the changes on the catalyst surface during O_2 treatment in the presence of AcOH.

DOI: 10.1021/acscatal.5b01140
ACS Catal. 2015, 5, 5776−5786

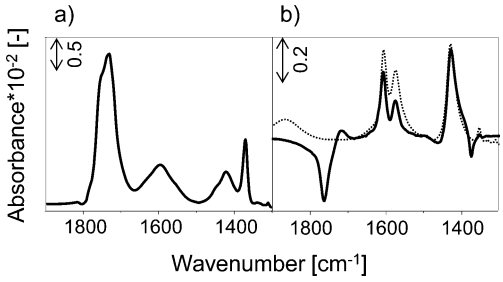

Figure 9. In situ IR spectra of Pd/SiO_2 adsorbed with (a) AcOH and (b) $AcOH/O_2$. The dotted curve in (b) represents the spectrum of $Pd(OAc)_2/SiO_2$. Adsorption conditions: 16 mbar of AcOH, 4.5 vol % of O_2, total flow of 20 mL/min; total pressure, 8.8 bar; temperature, 150 °C.

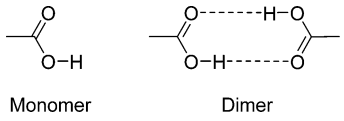

Figure 10. Structure of acetic acid monomer and dimer.

The bands at 1610 and 1576 cm^{-1} (ν_{as}(COO)) and at 1432 cm^{-1} (ν_s(COO) increased in intensity, while the ν(C═O) stretching vibration of AcOH at 1763 cm^{-1} decreased. This decrease cannot be attributed to the combustion of AcOH with O_2, because neither the formation of CO_2 nor the formation of carbonates was detected. Therefore, the decrease of ν(C═O) is attributed to the competitive adsorption of O_2 and to the formation of trimeric $Pd_3(OAc)_6$[88,95] (Figure 11a) and linear,

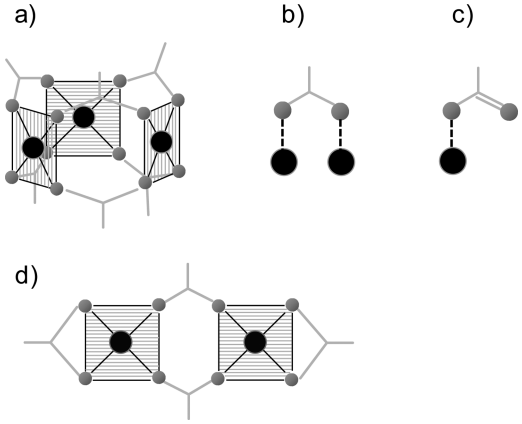

Figure 11. Structures of (a) trimeric $Pd_3(OAc)_6$ and (b) bridging (B) acetate on two Pd atoms, (c) terminal (T) acetate on Pd, and (d) dimeric $Pd_2(OAc)_4$. Black balls represent Pd and gray balls oxygen atoms.

dimeric ($Pd_2(OAc)_4$[95] (Figure 11d) dissolved in the acetic acid layer. The equilibrium between $Pd_3(OAc)_6$ and $Pd_2(OAc)_4$ in AcOH favors the former.[95] The increase in the corresponding symmetric and asymmetric COO stretching vibrations agrees perfectly with those of the $Pd(OAc)_2/SiO_2$ reference sample presented as a dotted curve in Figure 9b. However, acetate vibrations of $Pd(OAc)_2/SiO_2$ disappeared upon heating to 150 °C due to decomposition in the absence of AcOH. This suggests that $Pd_3(OAc)_6/Pd_2(OAc)_4$ are thermally stabilized only in the presence of AcOH. The structure of trimeric $Pd_3(OAc)_6$ is illustrated in Figure 11a,[96] where the acetate ligands are bound in a bridging (B) mode (Figure 11b) to two Pd sites with a square-planar configuration of Pd^{2+} (d^8). Figure 11c illustrates a terminal (T) acetate bound to Pd.

The IR spectrum of $PdAu/KOAc/SiO_2$ during AcOH adsorption at 150 °C and 9 bar total pressure is shown in Figure 12a. The surface concentration of AcOH on this

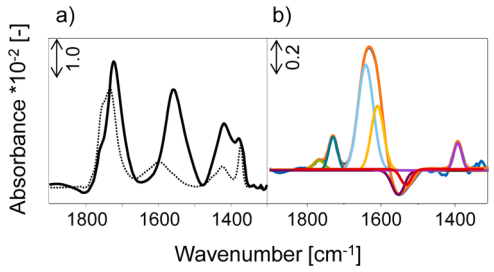

Figure 12. In situ IR spectra of $PdAu/KOAc/SiO_2$ adsorbed with (a) AcOH and (b) $AcOH/O_2$. The dotted curve in (a) indicates AcOH on Pd/SiO_2. Conditions: 16 mbar of AcOH, 4.5 vol % of O_2, total flow of 20 mL/min; total pressure, 8.8 bar; temperature, 150 °C.

promoted catalyst (ν(C═O) 1762, 1725 cm^{-1}) increased in comparison to Pd/SiO_2 (black dotted curve), which was caused by KOAc that retained additional AcOH. The high intensity of the ν(C═O) vibration located at 1725 cm^{-1} suggested the formation of dimeric $KOAc(HOAc)_n$ (n = 1, 2) species.[97] In addition, the presence of K^+ caused an overall conversion of AcOH to KOAc, demonstrated by the increasing intensity of acetate bands (ν_{as}(COO) 1500–1600 cm^{-1}, ν_s(COO) 1400–1480 cm^{-1};[98] Figure 12a).

The structural changes of the acetate species during exposure to the $AcOH/O_2$ mixture in comparison to pure AcOH are shown in Figure 12b. The bands at 1767 and 1730 cm^{-1} result from ν(C═O) of AcOH monomers and dimers. It should be noted that Augustine et al.[88] assigned the band at 1730 cm^{-1} to ν(C═O) of terminal acetate[16,99] bound to surface Pd atoms[100] or adsorbed AcOH.[11,101] The assignment to adsorbed AcOH appears unlikely, as the band at 1730 cm^{-1} hardly changed in intensity after purging with N_2. Thus, we conclude that terminal acetates are stabilized on Pd in Pd_xAu_y nanoparticles, which differ from the acetates in the molecular dissolved $Pd_3(OAc)_6$ because the ν_{as}(COO) vibration of the bridging acetates in $Pd_3(OAc)_6$ were found at 1610 cm^{-1}.[88] The terminal acetate species at 1730 cm^{-1} were not observed in the difference spectra of Pd/SiO_2 (Figure 9b), suggesting that KOAc favors the formation of these terminal acetates on PdAu. On $PdAu/KOAc/SiO_2$, a band at 1635 cm^{-1} appeared, in parallel to the decrease in intensity of the ν_{as}(COO) vibration of KOAc at 1575 cm^1. Augustine et al.[88] observed a similar band at 1651 cm^{-1} and assigned it to the ν(C═C) stretching vibrations in vinyl acetate, while the band was attributed to mixed "Li–Pd acetate" on a molecular Li–Pd acetate catalyst.[102] In the absence of ethene, the band at 1635 cm^{-1} cannot be caused by ν(C═C) vibrations in our studies. We assigned it, therefore, to a combination of bands arising from terminal acetates[16] at 1642 cm^{-1} and bridging acetates at 1610 cm^{-1}. The contributions were quantified by fitting the band at 1635 cm^{-1}. This ratio of terminal to bridging (T/B) acetates is characteristic for the different dimer species, as $K_2Pd_2(OAc)_6$, $KPd_2(OAc)_5$, and $Pd_2(OAc)_4$ exhibit ratios of 4/2, 2/3 and 0/4, respectively (Figure 13). The determined T/B ratio of 4/2 points to the formation of $K_2Pd_2(OAc)_6$ partially solved in the acetic acid layer. The presence of trimeric $Pd_3(OAc)_6$ and dimeric

DOI: 10.1021/acscatal.5b01140
ACS Catal. 2015, 5, 5776–5786

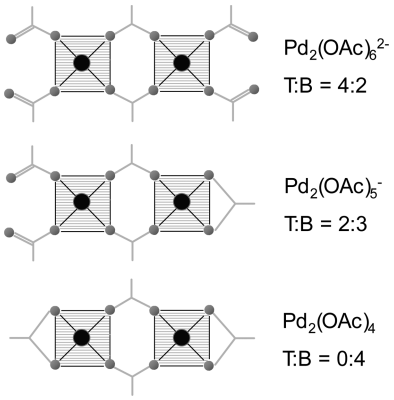

Figure 13. Dimeric palladium acetate species (T = terminal, B = bridging, bidentate acetate). Black balls denote Pd atoms and gray balls O atoms.

$Pd_2(OAc)_4$ was excluded, as both do not contain K^+ cations and have only bridging acetates. The $Pd_3(OAc)_6$ species formed were hypothesized to interact with KOAc[6,88] and to be essentially converted to dimeric species by KOAc.[14,16] Traces of unsaturated $KPd_2(OAc)_5$ (eq 3) with a T/B ratio of 2/3 could

$$2Pd_3(OAc)_6 + 3KOAc \rightleftharpoons 3KPd_2(OAc)_5 \quad (3)$$

not be excluded, as it is in equilibrium with $K_2Pd_2(OAc)_6$ (eq 4). Under the in situ conditions applied and the excess of

$$KPd_2(OAc)_5 + KOAc \rightleftharpoons K_2Pd_2(OAc)_6 \quad (4)$$

KOAc (overall Pd/K^+ ratio of 1/4) present in the promoted catalyst, we expect, however, that the equilibrium favors $K_2Pd_2(OAc)_6$. In agreement with this conclusion, studies of the homogeneous catalytic VA synthesis by palladium acetate in NaOAc/AcOH solution indicate $Na_2Pd_2(OAc)_6$ to be the active species that is converted to $NaPd_2(OAc)_5(C_2H_4)$ by attack of C_2H_4 (eq 5) to finally form Pd^0 and VA.[13,15,19]

$$Na_2Pd_2(OAc)_6 + C_2H_4 \rightleftharpoons NaPd_2(OAc)_5(C_2H_4) + NaOAc \quad (5)$$

In summary, KOAc retains AcOH on the catalyst and favors the formation of acetates, which are either transformed to terminal Pd acetates on the PdAu nanoparticle surface (active sites in the pathways catalyzed by the solid surface) or to $Pd_3(OAc)_6$ to create dimeric $K_2Pd_2(OAc)_6$ partially dissolved in the AcOH layer ($M_2Pd_2(OAc)_6$ as the active site/complex in the pathways catalyzed by a molecular catalyst[13,14]). The formation of homogeneous $K_2Pd_2(OAc)_6$ on the heterogeneous PdAu/KOAc catalyst and the presence of Pd acetate esters on the Pd_xAu_y surface indicate a direct link between these two pathways of catalyzed VA synthesis. Consequently, $K_2Pd_2(OAc)_6$ is proposed to be the key intermediate in the reordering process of PdAu nanoparticles.

3.3.2. Exploring the Catalysts in the Working State. While the conditions used so far allowed the qualitative and quantitative analysis of the surface states of the active nanoparticles and molecular complexes, the additional presence of ethene is expected to affect the equilibria, requiring a closer analysis of this situation.

The IR spectrum of the (unwashed) K^+-free PdAu/SiO_2 catalyst after reaction (SiO_2 support vibrations are subtracted) is shown in Figure 14a. The bands at 1785 and 1740 cm^{-1} are

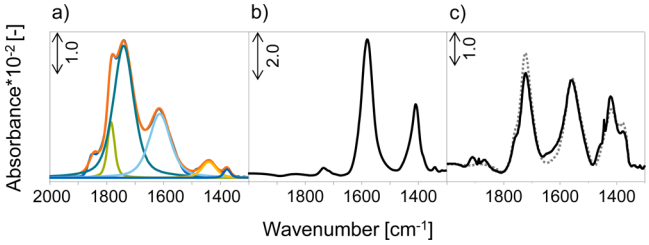

Figure 14. IR spectra of used, unwashed (a) PdAu/SiO_2 and (b) PdAu/KOAc/SiO_2 recorded at room temperature and (c) in situ IR spectra of PdAu/KOAc/SiO_2 adsorbed with AcOH (dotted curve) and with $AcOH/O_2/C_2H_4$ (solid curve). Adsorption conditions: 16 mbar of AcOH, 4.5 vol % of O_2, 60 vol % of C_2H_4; total flow of 20 mL/min; total pressure, 8.8 bar; temperature, 150 °C.

typical ν(C═O) vibrations of AcOH monomers and dimers. Asymmetric and symmetric carboxylate stretching vibrations of bridging acetates in trimeric $Pd_3(OAc)_6$ (Figure 11a) were observed at 1610 and 1436 cm^{-1}. Additionally, the orange-brown color of the washing water of PdAu/SiO_2 after the reaction points to the formation of $Pd_3(OAc)_6$. Thus, significant concentrations of $Pd_3(OAc)_6$ were stable under the reducing influence of 60 vol % of C_2H_4 during the reaction (150 °C and 9 bar total pressure). This agrees well with the fact that trimeric $Pd_3(OAc)_6$ is one of the most stable forms of Pd(II) acetate in solution.[16,95]

However, $Pd(OAc)_2$ impregnated on SiO_2 in the absence of AcOH started to decompose at ~150 °C. Thus, the thermal and reductive stability of $Pd_3(OAc)_6$ strongly depends on the presence and thickness of the acetic acid film, which we hypothesize to inhibit the reduction of $Pd_3(OAc)_6$ to Pd^0. To test this, PdAu/SiO_2 was quenched in C_2H_4 instead of N_2 after VA synthesis. Indeed, the colorless washing water of this PdAu/SiO_2 catalyst after the reaction contained black, dispersed Pd^0 particles from the reduction of $Pd_3(OAc)_6$ by C_2H_4 as soon as the protective AcOH layer was removed during quenching.

The IR spectrum of unwashed PdAu/KOAc/SiO_2 after the reaction is shown in Figure 14b. In contrast to PdAu/SiO_2, only KOAc vibrations (ν_{as}(COO) 1575 cm^{-1}, ν_s(COO) 1411 cm^{-1}) were observed, while bands of AcOH, $Pd_3(OAc)_6$, and $K_2Pd_2(OAc)_6$ were not found. We conclude that AcOH desorbed completely during 2 h of purging with N_2 at 150 °C. The absence of $Pd_3(OAc)_6$ is reasonable, as KOAc shifts the equilibrium (eq 1) to the side of $K_2Pd_2(OAc)_6$, as observed experimentally on PdAu/KOAc/SiO_2 during $AcOH/O_2$ adsorption.

In order to study PdAu/KOAc/SiO_2 under reaction conditions, Figure 14c compares the in situ IR spectra of PdAu/KOAc/SiO_2 adsorbed with AcOH (black dotted curve) and with $AcOH/O_2/C_2H_4$ (black curve). Bands for the CH_2 out-of-plane (1888 cm^{-1}) and the CH_2 in-plane (1445 cm^{-1}) deformation vibrations of C_2H_4 are present.[103,104] Asymmetric carboxylate stretching vibrations of terminal acetates at 1642 cm^{-1} and small amounts of bridging acetates at 1611 cm^{-1} confirm the presence of far less $K_2Pd_2(OAc)_6$ species during reducing $AcOH/O_2/C_2H_4$ treatment in comparison to that in oxidizing $AcOH/O_2$ (Figure 12b).

The reason for the absence of $K_2Pd_2(OAc)_6$ bands on PdAu/KOAc/SiO_2 after the reaction and the presence of

DOI: 10.1021/acscatal.5b01140
ACS Catal. 2015, 5, 5776−5786

$K_2Pd_2(OAc)_6$ during $AcOH/O_2/C_2H_4$ treatment to a lesser extent than during $AcOH/O_2$ treatment could be the facile reduction and decomposition of $K_2Pd_2(OAc)_6$ to Pd^0. Nakamura et al.[6] reported that Pd acetate with KOAc was easily reduced to Pd black by forming VA, while Pd acetate alone did not react. They concluded that KOAc weakens Pd−O bonds in Pd acetate,[6] which agrees with the present observation of the $K_2Pd_2(OAc)_6$ intermediate, while $Pd_3(OAc)_6$ was not formed. In fact, Pandey et al. suggested that bridging acetates in $Pd_3(OAc)_6$ are far less reactive toward olefins than the (labile) terminal acetates in dimeric $K_2Pd_2(OAc)_6$.[13,14,16]

In order to test the differences in reducibility of $K_2Pd_2(OAc)_6$ and $Pd_3(OAc)_6$, silica-supported $Pd(OAc)_2$ and $Pd(OAc)_2$/KOAc were used as catalysts, following the formation of Pd^0 particles by XRD (Figure S5 in the Supporting Information). The full width at half-maximum of Pd reflections from $Pd(OAc)_2$/KOAc was generally smaller than those of unpromoted $Pd(OAc)_2$. The deduced formation of larger particles points to the lower stability of $K_2Pd_2(OAc)_6$ in comparison to $Pd_3(OAc)_6$. Thus, we hypothesize that the addition of promoter acetates also increases the contribution of the molecularly catalyzed pathway of VA synthesis.[105]

3.4. Dynamic Reconstruction of KOAc Promoted and Unpromoted PdAu/SiO_2. Pd-containing particles on fresh $PdAu/SiO_2$ deplete in Pd by oxidative leaching of $Pd_3(OAc)_6$ into the acetic acid layer. This layer protects $Pd_3(OAc)_6$ from decomposition and reduction. Thus, reincorporation of Pd^0 formed by reduction of $Pd_3(OAc)_6$ with ethene into PdAu particles is not favored.[6] Consequently, Au-enriched PdAu particles are formed (Figure 15).

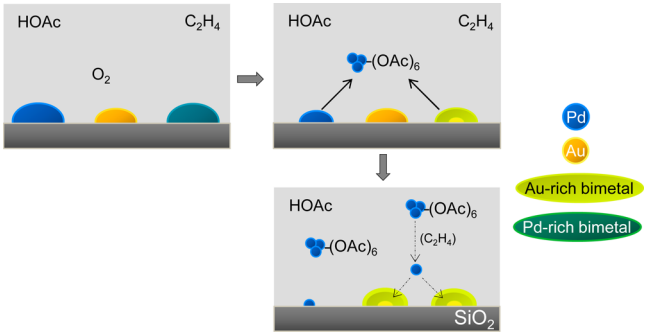

Figure 15. Proposed reordering mechanism of $PdAu/SiO_2$ during VA synthesis. Pd is represented in blue and Au in yellow, and the bimetallic PdAu particles are represented in green.

Fresh $PdAu/KOAc/SiO_2$ contains Pd- and Au-rich and $Pd_{54}Au_{46}$ bimetallic particles. KOAc adsorbed on PdAu particles leads to the migration of Pd from the bulk to the surface and finally to oxidative leaching of mixed $K_2Pd_2(OAc)_6$. In contrast to the case for $Pd_3(OAc)_6$, $K_2Pd_2(OAc)_6$ is easily reduced by ethene to Pd^0, which either forms dispersed Pd^0 clusters in AcOH or reincorporates into the PdAu particles to maintain the stable Pd_1Au_1 bulk phase with a Pd-enriched PdAu surface (Figure 16).

4. CONCLUSIONS

KOAc promotion of bimetallic $PdAu/SiO_2$ enhanced the activity by a factor of 10 and the selectivity by approximately 20%. In the absence of KOAc, trimeric $Pd_3(OAc)_6$ is oxidatively leached from the bimetallic particles into the AcOH layer. AcOH stabilized $Pd_3(OAc)_6$ against reduction by ethene, thus

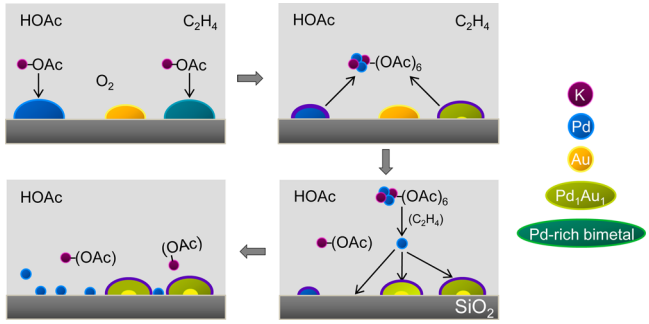

Figure 16. Proposed reordering mechanism of $PdAu/KOAc/SiO_2$ during VA synthesis. Pd is represented in blue, Au in yellow, and K^+ in violet, and the bimetallic PdAu particles are represented in green.

lowering the probability for Pd^0 to reincorporate into PdAu particles. Consequently, Pd_1Au_1-enriched nanoparticles form the bulk of the supported particles. The low activity and selectivity of unpromoted $PdAu/SiO_2$ are attributed to the low Pd concentration on the Au-rich bimetallic surfaces, favoring decomposition to CO_2 and H_2O rather than VA formation.

Potassium (in the form of K^+) is located in the acetic acid film as well as on the PdAu particles, where it acts as an electronic promoter for Pd and Au and as an agent to stabilize Pd on the surface of the bimetallic particles forming the active sites. Strong interactions between K^+ and Pd led to the formation of dimeric $K_2Pd_2(OAc)_6$ species, acting as an organometallic catalyst in the condensed AcOH layer. KOAc transfers acetates to Pd, thereby increasing the acetate concentration for the rate-determining step to VA. The probability for ethylene to adsorb and combust is thus statistically lowered, increasing the selectivity VA.

■ ASSOCIATED CONTENT

Supporting Information

The Supporting Information is available free of charge on the ACS Publications website at DOI: 10.1021/acscatal.5b01140.

Additional information on transmission electron microscopy, IR spectra of adsorbed CO at −150 °C, calculation of the absorption coefficients of CO on Au and Pd, and X-ray profiles (PDF)

■ AUTHOR INFORMATION

Corresponding Author

*J.A.L.: e-mail, johannes.lercher@mytum.de; tel, 0049 89 289 13540; fax, 0049 89 289 13544.

Notes

The authors declare no competing financial interest.

■ ACKNOWLEDGMENTS

Financial support by Wacker Chemie AG and fruitful discussions within the Wacker-Institut für Siliciumchemie is gratefully acknowledged. Xaver Hecht and Martin Neukamm are acknowledged for their experimental support.

■ REFERENCES

(1) Han, Y. F.; Wang, J. H.; Kumar, D.; Yan, Z.; Goodman, D. W. *J. Catal.* **2005**, *232*, 467−475.

(2) Ertl, G.; Knözinger, H.; Weitkamp, J. *Handbook of Heterogeneous Catalysis*; Wiley-VCH: Weinheim, Germany, 1997; Vol. 5, pp 2295−2298.

(3) Chen, M.; Kumar, D.; Yi, C.-W.; Goodman, D. W. *Science* **2005**, *310*, 291−293.

DOI: 10.1021/acscatal.5b01140
ACS Catal. 2015, 5, 5776−5786

(4) Pohl, M.-M.; Radnik, J.; Schneider, M.; Bentrup, U.; Linke, D.; Brückner, A.; Ferguson, E. *J. Catal.* **2009**, *262*, 314−323.
(5) Simson, S.; Jentys, A.; Lercher, J. A. *J. Phys. Chem. C* **2013**, *117*, 8161−8169.
(6) Nakamura, S.; Yasui, T. *J. Catal.* **1970**, *17*, 366−374.
(7) Koukiou, S.; Konsolakis, M.; Lambert, R. M.; Yentekakis, I. V. *Appl. Catal., B* **2007**, *76*, 101−106.
(8) Pitchon, V.; Guenin, M.; Praliaud, H. *Appl. Catal.* **1990**, *63*, 333−343.
(9) Tom, H. W. K.; Mate, C. M.; Zhu, X. D.; Crowell, J. E.; Shen, Y. R.; Somorjai, G. A. *Surf. Sci.* **1986**, *172*, 466−476.
(10) Gravelle-Rumeau-Maillot, M.; Pitchon, V.; Martin, G. A.; Praliaud, H. *Appl. Catal., A* **1993**, *98*, 45−59.
(11) Crathorne, E. A.; Macgowan, D.; Morris, S. R.; Rawlinson, A. P. *J. Catal.* **1994**, *149*, 254−267.
(12) Brown, R. G.; Davidson, J. M.; Triggs, C. *Am. Chem. Soc., Div. Petrol. Chem.* **1969**, *14*, B23−B28.
(13) Pandey, R. N.; Henry, P. M. *Can. J. Chem.* **1975**, *53*, 1833−1841.
(14) Pandey, R. N.; Henry, P. M. *Can. J. Chem.* **1974**, *52*, 1241−1247.
(15) Kragten, D. D.; van Santen, R. A.; Neurock, M.; Lerou, J. J. *J. Phys. Chem. A* **1999**, *103*, 2756−2765.
(16) Kragten, D. D.; van Santen, R. A.; Crawford, M. K.; Provine, W. D.; Lerou, J. J. *Inorg. Chem.* **1999**, *38*, 331−339.
(17) Bancroft, D. P.; Cotton, F. A.; Falvello, L. R.; Schwotzer, W. *Polyhedron* **1988**, *7*, 615−621.
(18) Skapski, A. C.; Smart, M. L. *J. Chem. Soc. D* **1970**, 658b−659b.
(19) Winstein, S.; McCaskie, J.; Lee, H.-B.; Henry, P. M. *J. Am. Chem. Soc.* **1976**, *98*, 6913−6918.
(20) Somorjai, G. A.; Contreras, A. M.; Montano, M.; Rioux, R. M. *Proc. Natl. Acad. Sci. U. S. A.* **2006**, *103*, 10577−10583.
(21) Eberle, H.-J.; Heidenreich, R.; Weis, J. German Patent DE 10 2006 058 800 A1, 2008.06.19, 2008, 1−18.
(22) Vegard, L. *Eur. Phys. J. A* **1921**, *5*, 17−26.
(23) Mirth, G.; Eder, F.; Lercher, J. A. *Appl. Spectrosc.* **1994**, *48*, 194−197.
(24) Provine, W. D.; Mills, P. L.; Lerou, J. J. *Stud. Surf. Sci. Catal.* **1996**, *101*, 191−200.
(25) Thompson, D. T. *Platinum Met. Rev.* **2004**, *48*, 169−172.
(26) Han, Y. F.; Kumar, D.; Goodman, D. W. *J. Catal.* **2005**, *230*, 353−358.
(27) Voskanyan, P. S. *Catal. Ind.* **2010**, *2*, 167−172.
(28) Reifsnyder, S. N.; Lamb, H. H. *J. Phys. Chem. B* **1999**, *103*, 321−329.
(29) Davis, R. J.; Boudart, M. *J. Phys. Chem.* **1994**, *98*, 5471−5477.
(30) Macleod, N.; Keel, J. M.; Lambert, R. M. *Appl. Catal., A* **2004**, *261*, 37−46.
(31) Smejkal, Q.; Linke, D.; Bentrup, U.; Pohl, M. M.; Berndt, H.; Baerns, M.; Brückner, A. *Appl. Catal., A* **2004**, *268*, 67−76.
(32) Pellegrini, R.; Leofanti, G.; Agostini, G.; Bertinetti, L.; Bertarione, S.; Groppo, E.; Zecchina, A.; Lamberti, C. *J. Catal.* **2009**, *267*, 40−49.
(33) Allison, E. G.; Bond, G. C. *Catal. Rev.: Sci. Eng.* **1972**, *7*, 233−289.
(34) Okamoto, H.; Massalski, T. *Bull. Alloy Phase Diagrams* **1985**, *6*, 229−235.
(35) Oriani, R.; Murphy, W. K. *Acta Metall.* **1962**, *10*, 879−885.
(36) Wolf, A.; Schüth, F. *Appl. Catal., A* **2002**, *226*, 1−13.
(37) Liu, X.; Wang, A.; Zhang, T.; Su, D.-S.; Mou, C.-Y. *Catal. Today* **2011**, *160*, 103−108.
(38) Wang, A.; Liu, X. Y.; Mou, C.-Y.; Zhang, T. *J. Catal.* **2013**, *308*, 258−271.
(39) Kuhn, W. K.; Szanyi, J.; Goodman, D. W. *Surf. Sci.* **1992**, *274*, L611−L618.
(40) Mihaylov, M.; Hadjiivanov, K.; Knözinger, H. *Catal. Lett.* **2001**, *76*, 59−63.
(41) Montanari, T.; Castoldi, L.; Lietti, L.; Busca, G. *Appl. Catal., A* **2011**, *400*, 61−69.
(42) Montanari, T.; Matarrese, R.; Artioli, N.; Busca, G. *Appl. Catal., B* **2011**, *105*, 15−23.
(43) Beebe, T. P.; Gelin, P.; Yates, J. T., Jr *Surf. Sci.* **1984**, *148*, 526−550.
(44) Mihaylov, M.; Knözinger, H.; Hadjiivanov, K.; Gates, B. C. *Chem. Ing. Tech.* **2007**, *79*, 795−806.
(45) Vannice, M. A.; Wang, S. Y. *J. Phys. Chem.* **1981**, *85*, 2543−2546.
(46) Eischens, R. P.; Francis, S. A.; Pliskin, W. A. *J. Phys. Chem.* **1956**, *60*, 194−201.
(47) Shen, J.; Hill, J.; Watwe, R.; Podkolzin, S. G.; Dumesic, J. A. *Catal. Lett.* **1999**, *60*, 1−9.
(48) Kugler, E. L.; Boudart, M. *J. Catal.* **1979**, *59*, 201−210.
(49) Meier, D. C.; Goodman, D. W. *J. Am. Chem. Soc.* **2004**, *126*, 1892−1899.
(50) Chen, M. S.; Luo, K.; Wei, T.; Yan, Z.; Kumar, D.; Yi, C. W.; Goodman, D. W. *Catal. Today* **2006**, *117*, 37−45.
(51) Ozensoy, E.; Wayne Goodman, D. *Phys. Chem. Chem. Phys.* **2004**, *6*, 3765−3778.
(52) Wei, T.; Wang, J.; Goodman, D. W. *J. Phys. Chem. C* **2007**, *111*, 8781−8788.
(53) Gao, F.; Goodman, D. W. *Chem. Soc. Rev.* **2012**, *41*, 8009−8020.
(54) Angevaare, P. A. J. M.; Hendrickx, H. A. C. M.; Ponec, V. *J. Catal.* **1988**, *110*, 11−17.
(55) Lang, N. D.; Williams, A. R. *Phys. Rev. Lett.* **1976**, *37*, 212−215.
(56) Lang, N. D.; Williams, A. R. *Phys. Rev. B: Condens. Matter Mater. Phys.* **1978**, *18*, 616−636.
(57) Gadzuk, J. W. *Surf. Sci.* **1967**, *6*, 133−158.
(58) Praliaud, H.; Primet, M.; Martin, G.-A. *Appl. Surf. Sci.* **1983**, *17*, 107−123.
(59) Liotta, L. F.; Martin, G. A.; Deganello, G. *J. Catal.* **1996**, *164*, 322−333.
(60) Crowell, J. E.; Garfunkel, E. L.; Somorjai, G. A. *Surf. Sci.* **1982**, *121*, 303−320.
(61) Blyholder, G. *J. Phys. Chem.* **1964**, *68*, 2772−2777.
(62) Campbell, C. T.; Goodman, D. W. *Surf. Sci.* **1982**, *123*, 413−426.
(63) Garfunkel, E. L.; Crowell, J. E.; Somorjai, G. A. *J. Phys. Chem.* **1982**, *86*, 310−313.
(64) Gusovius, A. F.; Watling, T. C.; Prins, R. *Appl. Catal., A* **1999**, *188*, 187−199.
(65) Pitchon, V.; Primet, M.; Praliaud, H. *Appl. Catal.* **1990**, *62*, 317−334.
(66) Uram, K. J.; Ng, L.; Folman, M.; Yates, J. T. *J. Chem. Phys.* **1986**, *84*, 2891−2895.
(67) Dose, V.; Rogozik, J.; Bradshaw, A. M.; Prince, K. C. *Surf. Sci.* **1987**, *179*, 90−100.
(68) Mott, N. F. *Proc. Phys. Soc.* **1935**, *47*, 571−588.
(69) Liu, P.; Nørskov, J. K. *Phys. Chem. Chem. Phys.* **2001**, *3*, 3814−3818.
(70) Couper, A.; Eley, D. D. *Discuss. Faraday Soc.* **1950**, *8*, 172−184.
(71) Kim, M. J.; Flanagan, W. F. *Acta Metall.* **1967**, *15*, 747−752.
(72) Rodriguez, J. A.; Goodman, D. W. *Science* **1992**, *257*, 897−903.
(73) Lee, Y.-S.; Jeon, Y.; Chung, Y.-M.; Lim, K.-Y.; Whang, C.-N.; Oh, S.-J. *J. Korean Phys. Soc.* **2000**, *37*, 451−455.
(74) Christensen, A.; Ruban, A. V.; Stoltze, P.; Jacobsen, K. W.; Skriver, H. L.; Nørskov, J. K.; Besenbacher, F. *Phys. Rev. B: Condens. Matter Mater. Phys.* **1997**, *56*, 5822−5834.
(75) Varga, P.; Hetzendorf, G. *Surf. Sci.* **1985**, *162*, 544−549.
(76) Maire, G.; Hilaire, L.; Legare, P.; Gault, F. G.; O'Cinneide, A. *J. Catal.* **1976**, *44*, 293−299.
(77) Luo, K.; Wei, T.; Yi, C. W.; Axnanda, S.; Goodman, D. W. *J. Phys. Chem. B* **2005**, *109*, 23517−23522.
(78) Yi, C. W.; Luo, K.; Wei, T.; Goodman, D. W. *J. Phys. Chem. B* **2005**, *109*, 18535−18540.
(79) Mejía-Rosales, S. J.; Fernández-Navarro, C.; Pérez-Tijerina, E.; Montejano-Carrizales, J. M.; José-Yacamán, M. *J. Phys. Chem. B* **2006**, *110*, 12884−12889.
(80) Mezey, L. Z.; Giber, J. *Jpn. J. Appl. Phys.* **1982**, *21*, 1569−1571.

DOI: 10.1021/acscatal.5b01140
ACS Catal. 2015, 5, 5776−5786

(81) Anton, R.; Eggers, H.; Veletas, J. *Thin Solid Films* **1993**, *226*, 39−47.
(82) Rainer, D. *J. Vac. Sci. Technol., A* **1997**, *15*, 1653−1662.
(83) Swartzfager, D. G.; Ziemecki, S. B.; Kelley, M. J. *J. Vac. Sci. Technol.* **1981**, *19*, 185−191.
(84) Chen, M.; Goodman, D. W. *Chin. J. Catal.* **2008**, *29*, 1178−1186.
(85) Yuan, D.; Gong, X.; Wu, R. *J. Phys. Chem. C* **2008**, *112*, 1539−1543.
(86) Beck, I. E.; Gusevskaya, E. V.; Stepanov, A. G.; Likholobov, V. A. *J. Mol. Catal.* **1992**, *73*, 115−146.
(87) Weltner, W. *J. Am. Chem. Soc.* **1955**, *77*, 3941−3950.
(88) Augustine, S. M.; Blitz, J. P. *J. Catal.* **1993**, *142*, 312−324.
(89) Liao, L.-F.; Lien, C.-F.; Lin, J.-L. *Phys. Chem. Chem. Phys.* **2001**, *3*, 3831−3837.
(90) Hill, W.; Miessner, H.; Ohlmann, G. *J. Chem. Soc., Faraday Trans. 1* **1989**, *85*, 691−697.
(91) Jackson, S. D.; Kelly, G. J.; Lennon, D. *React. Kinet. Catal. Lett.* **2000**, *70*, 207−212.
(92) Alcock, N. W.; Tracy, V. M.; Waddington, T. C. *J. Chem. Soc., Dalton Trans.* **1976**, 2243−2246.
(93) Stephenson, T. A.; Morehouse, S. M.; Powell, A. R.; Heffer, J. P.; Wilkinson, G. *J. Chem. Soc.* **1965**, 3632−3640.
(94) Fujimoto, K.; Negami, Y.; Takahashi, T.; Kunugi, T. *Ind. Eng. Chem. Prod. Res. Dev.* **1972**, *11*, 303−308.
(95) Stoyanov, E. *J. Struct. Chem.* **2000**, *41*, 440−445.
(96) Hollemann, A. F.; Wiberg, N. *Lehrbuch der Anorganischen Chemie*; Walter de Gruyter: Berlin, New York, 1995; pp 1598−1598.
(97) Davidson, A. W.; McAllister, W. H. *J. Am. Chem. Soc.* **1930**, *52*, 507−519.
(98) Ito, K.; Bernstein, H. J. *Can. J. Chem.* **1956**, *34*, 170−178.
(99) Haley, R. D.; Tikhov, M. S.; Lambert, R. M. *Catal. Lett.* **2001**, *76*, 125−130.
(100) Pei, Z. F.; Ponec, V. *Appl. Surf. Sci.* **1996**, *103*, 171−182.
(101) Kubicki, J. D.; Schroeter, L. M.; Itoh, M. J.; Nguyen, B. N.; Apitz, S. E. *Geochim. Cosmochim. Acta* **1999**, *63*, 2709−2725.
(102) Zaidi, S. A. H. *Appl. Catal.* **1988**, *38*, 353−358.
(103) Smith, A. W. J.; Poulston, S.; Rowsell, L. *Platinum Met. Rev.* **2009**, *53*, 112−122.
(104) Bernardet, V.; Decrette, A.; Simon, J.-M.; Bertrand, O.; Weber, G.; Bellat, E.-P. *Adsorption* **2005**, *11*, 383−389.
(105) van Helden, R.; Kohll, C. F.; Medema, D.; Verberg, G.; Jonkhoff, T. *Recl. Trav. Chim. Pays-Bas* **1968**, *87*, 961−991.

DOI: 10.1021/acscatal.5b01140
ACS Catal. 2015, 5, 5776−5786